Evaluation of Fly Ash-based Alkali Activated Foams at Room and Elevated Temperatures

Katja Traven[1], Mark Češnovar[1,2], Srečo Škapin[3] & Vilma Ducman[1]

[1] Slovenian National Building and Civil Engineering Institute, Department for Materials, Ljubljana, Slovenia, e-mail: katja.traven@zag.si, mark.cesnovar@zag.si, vilma.ducman@zag.si

[2] International Postgraduate School Jožef Stefan, Ljubljana, Slovenia, e-mail: mark.cesnovar@zag.si

[3] Jožef Stefan Institute, Ljubljana, Slovenia, e-mail: sreco.skapin@ijs.si

Abstract Alkali activated materials (AAM) are, in their broadest classification, any binder systems derived by the reaction of an alkali metal source (silicates, alkali hydroxides, carbonates, sulphates) with a solid, amorphous alumosilicate powder (found in precursors such as slag, fly ash and bottom ash). A wide variety of products can be obtained by the alkali activation process and could replace traditional construction products. Among these, alkali activated foams (AAF) represent one of the most promising materials, owing to their economically accessible alumosilicate rich source materials, including industrial waste materials, clean processing, higher added value and most importantly, products with competitive properties. In the present study, the properties of alkali activated fly ash-based foam materials were studied at room temperature as well as at elevated temperatures (up to 1200 °C) in order to develop a durable material in terms of mechanical properties and suitability for high temperature applications.

1   Introduction

Alkali-activated materials (AAM), also known as geopolymers or inorganic polymers, in their broadest classification, are any binder systems derived by the reaction of a liquid alkali metal source (silicates, alkali hydroxides, carbonates, sulphates) with a solid, amorphous aluminosilicate powder found in various precursors such as slag, fly ash and bottom ash. When the two components (activator and precursor) are mixed, dissolution and transport of the Al and Si atoms in the alkaline activators takes place first, and then an aluminosilicate network is formed through the poly-condensation of the Al and Si, which can again be amorphous or partially crystallized (Provis & van Deventer, 2013). Besides the chemical composition and the presence of amorphous alumosilicates in precursors as the main requirement for alkali activation, there are several influential parameters that can significantly affect the final mechanical and microstructural properties of the material: the curing regime and ageing (Češnovar *et al.*, 2019), particle size distribution (Traven *et al.*, 2019), type of activator (Chen *et al.*, 2017), Si/Al ratio (Duxson *et al.*, 2005), pH value (Khale & Chaudhary, 2007)**,** etc. Owing to the wide variety of suitable precursors, AAM could be designed to have properties superior to those of conventional binders (Aiken *et al.*, 2017)**,** and when waste material is used as a precursor/activator and a low temperature process is adopted, a reduction of the CO_2 footprint can also be achieved (van Deventer *et al.*, 2012).

A wide variety of products that can be obtained by the alkali activation process (such as blocks, slabs, paving stones, curbs, partitions, refractory materials, materials for specific industrial applications, etc.), and these could replace traditional construction products. Among them, alkali-activated foams (AAF) represent one of the most promising materials to be used as an insulating material in building and construction, on account of their potentially higher added value. The advantage of such materials in comparison with glass or ceramics lies in the lower processing temperatures (up to 100 °C) required to achieve properties similar to those of foamed glass or ceramics, both of which are produced at highly elevated temperatures (above 900 °C). AAF are formed with air voids introduced to a slurry that could be implemented either mechanically, where the alkali-activated material is physically mixed with premade foam, or chemically, using foaming agents such as aluminium (Al), silicon powders, SiC, FeSi alloy, hydrogen peroxide (H_2O_2), NaOCl, sodium perborate, etc. In this case, the chemical blowing agents form gaseous products (such

K. Traven, M. Češnovar, S. Škapin & V. Ducman:
Foundry Wastes as a Potential Precursor in Alkali Activation Technology

25

as O_2 or H_2) and other by-products by thermal decomposition or chemical reaction, as follows (for selected foaming agents):

$$2Al\ (s) + 2MOH\ (aq) + 2H_2O\ (l) \rightarrow 2MAlO_2\ (aq) + 3H_2\ (g) \qquad (1)$$

$$2H_2O_2\ (l) \rightarrow 2H_2O\ (g) + O_2\ (g) \qquad (2)$$

The gas bubbles generated either mechanically or chemically are incorporated into the slurry, and when suitable amounts of foaming agent are added, the material is highly porous. Furthermore, stabilizing agents or surfactants can be added to the slurry to decrease the surface tension of the air/slurry system and therefore stabilize the wet foam by reducing the coalescence of bubbles (Korat & Ducman, 2017). The surfactants can be divided into anionic (e.g. sodium oleate, sodium dodecyl sulphate), non-ionic (e.g. Triton X 100) or cationic. This leads to their diverse characteristics and consequently influences the morphology and pore architecture of the foams (Bai & Colombo, 2018). Regardless of the foaming method and/or the type of stabilizing agent, the compressive strength of AAF decreases with a reduction in density and is usually between 1 MPa and 10 MPa in the density range of 360–1400 kg/m³ (Zhang *et al.*, 2014).

In the present study, alkali-activated fly ash-based foam materials were studied in order to develop a durable material in terms of mechanical properties. Samples were assessed for their dimensional stability and thermal resistance, as well as their mechanical/microstructural properties after treatment at 600, 800, 1000 and 1200 °C. Furthermore, these properties directly follow the microstructure of AAF, which is affected by the composition and density (porosity).

2 Experimental

2.1 Materials and AAM/AAF preparation

Fly ash (FA) was obtained from the Thermal Power Plant Šoštanj (Slovenia) and was first characterized by means of XRF, XRD and SEM. The chemical composition of the investigated FA is shown in Table 1, and the results of the mineralogical analysis, along with SEM characterization are shown in Figure 1. Water glass (potassium silicate Betol K 5020 T, produced by Woellner Austria GmbH; $SiO_2{:}K_2O =$
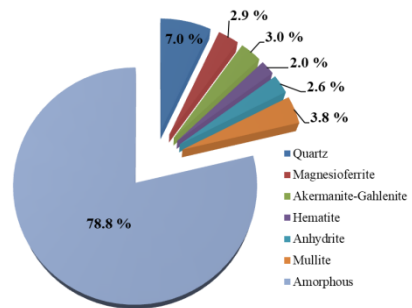
1.63 mass %; 51.5 mass % aqueous solution) and/or NaOH (produced by Donau Chemie, solid or 41.7 mass % water solution) were used as activators.
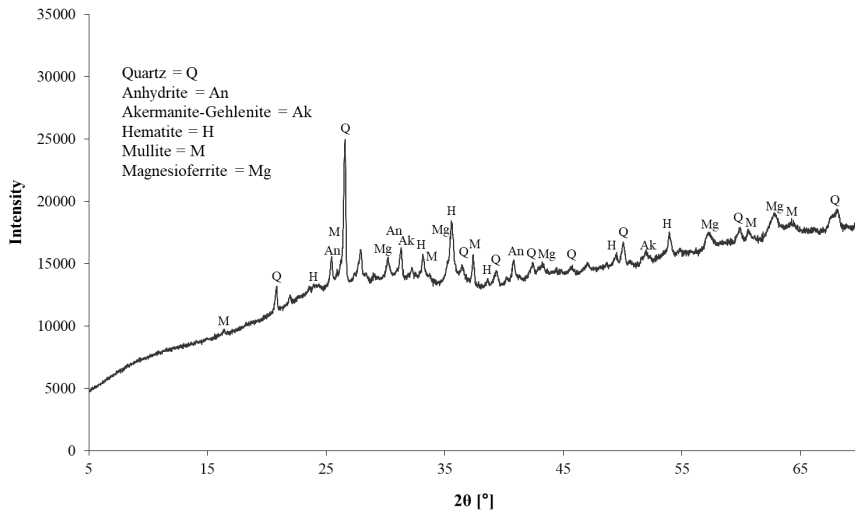
Table 1: Chemical composition of fly ash.

	LOI	Na$_2$O	MgO	Al$_2$O$_3$	SiO$_2$	P$_2$O$_5$	SO$_3$	K$_2$O	CaO	Fe$_2$O$_3$	OTH
Fly ash	0.51	1.19	2.80	22.98	44.82	0.36	0.77	2.20	12.38	10.65	1.34
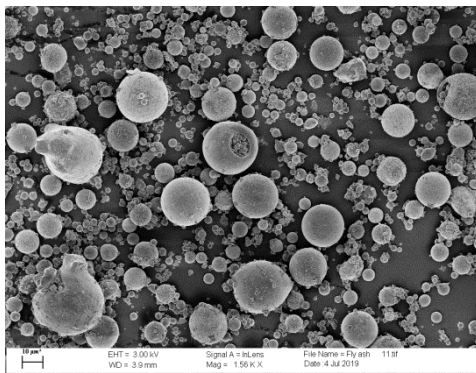
a)   b)

c)

Figure 1: Scanning electron microscopy (SEM) image of FA (a); identified phases in FA with their distribution in % (b) and X-ray diffractogram of FA (c).

K. Traven, M. Češnovar, S. Škapin & V. Ducman:
Foundry Wastes as a Potential Precursor in Alkali Activation Technology

27

After analysis of the source material, AAM mixtures with different FA/activator ratios were prepared and designated as shown in Table 2. Mechanical strengths were determined 3 days after curing at a temperature of 70 °C. The mixture showing best performance in terms of mechanical (flexural and compressive) strength (i.e. FA3) was further used for the development of lightweight AAF foamed with 1 mass % of H_2O_2 (hereafter denoted as FA3f). Pores were stabilized with the addition of 1 mass % of sodium dodecyl sulphate (SDS) as a surfactant. The freshly foamed pastes were poured into $20 \times 20 \times 80$ mm³ moulds and cured at 70 °C for 3 days. The hardened AAF (specimen AF3f) were then exposed to elevated temperatures (600, 800, 1000 and 1200 °C; hereafter denoted as FA3f 600, FA3f 800, FA3f 1000 and FA3f 1200, respectively) in order to study their dimensional stability, thermal resistance properties as well as their mechanical and microstructural properties after the heat treatment. The density of all AAF was determined by weighing the individual foams and dividing the resulting weights by the corresponding dimensions of the specimens (i.e. geometrical density).

Table 2: Composition of different mixtures prepared for the investigation (all in mass %) with the calculated (Na+K)/Al/Si ratios in prepared mixtures.

Sample designation	FA	Na_2SiO_3	NaOH	(Na+K)/Al/Si ratio in prepared mixture
FA1	0.71	0.29	/	0.79/1/2.0
FA2	0.85	/	0.15	1.3/1/1.53
FA3	0.73	0.24	0.03	0.91/1/1.93

2.2 Characterization methods and instruments

The chemical composition of the precursors was determined using a Wavelength Dispersive X-ray Fluorescence (WD XRF) analyser, manufactured by Thermo Scientific ARL Perform X. Mechanical strength (flexural and compressive strength) was determined at 3 days by means of Toninorm test equipment (Toni Technik, Germany), using a force application rate of 0.005 kN/s. XRD of FA was determined using a PANalytical Empyrean X-ray diffractometer with CuKα radiation ($\lambda = 1.54$ Å) at a voltage of 45 kV and a current of 40 mA, in the 2θ range from 4° to 70° (scan rate = 0.026°/min). Data was then analysed with X'Pert High Score

Plus diffraction software (PANalytical), using the database PDF 4+2015 RDB powder diffraction files. Rietveld refinement was performed by X'Pert High Score Plus diffraction software. XRD of AAF was determined using D4 Endeavour, Bruker AXS, Karlsruhe (Germany). Dilatometric analysis was performed by means of a Dilatometer Netzsch DIL 402 up to 1000 °C with a heating rate of 5°/min. Microstructural analysis of the precursor as well as hardened AAF was performed by an Ultra plus FESEM, Carl Zeiss (Germany).

3   Results and discussion

The present study was primarily focused on precursor (FA) characterization in order to determine the suitability for alkali activation. According to the XRD analysis, the presence of quartz, magnesioferrite, akermanite-gehlenite, hematite, anhydrite and mullite was confirmed, as well as over 70 % of the amorphous phase needed for the alkali activation process (Figs. 1b and 1c). The presence of favourable alumosilicates was also confirmed by the chemical analysis presented in Table 1. Scanning Electron Microscopy (SEM) was conducted to investigate the morphology of particles (Fig. 1a), which in this case are generally spherical, with a diameter ranging from 1 μm up to 20 μm.
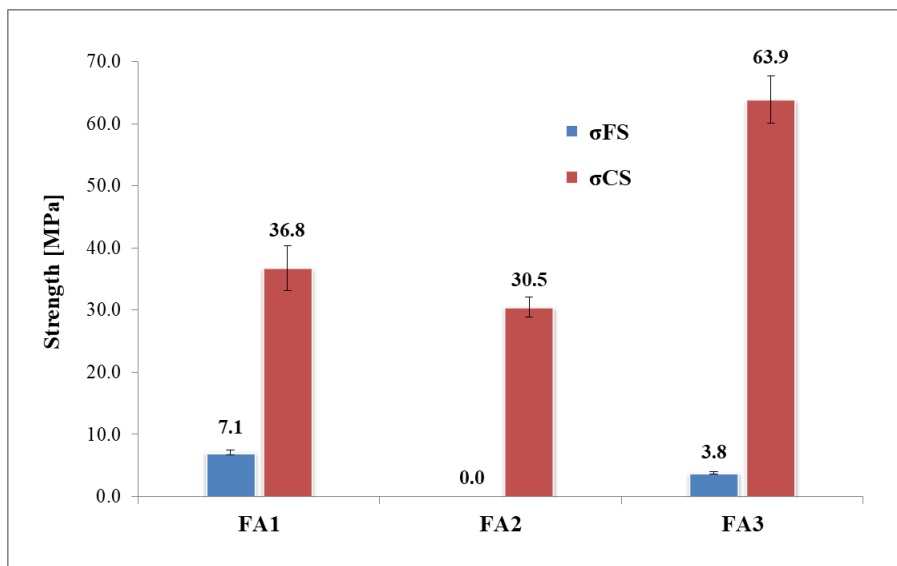

Figure 2: Flexural (σ_{FS}) and compressive (σ_{CS}) strength of different AAM mixtures.

K. Traven, M. Češnovar, S. Škapin & V. Ducman:
Foundry Wastes as a Potential Precursor in Alkali Activation Technology

29

To achieve optimal mechanical strengths of hardened AAM, in the next stage of the study focused on the influence of the precursor/activator solution mix ratio. Three mixtures were prepared (Table 2), also taking into account the (Na+K)/Al/Si ratios. Theoretically, the ideal ratio for achieving the best mechanical strength performance is found to be 1/1/1.9 (Duxson *et al.*, 2005). Based on results for the mechanical properties presented in Figure 2, sufficient flexural strength and the maximum compressive strength were found in the case of mixture FA3, which was thus selected for the further development of lightweight AAF. Among all three, the FA3 specimen also exhibited the closest (Na+K)/Al/Si ratio in comparison to the theoretical calculations (Table 2).

In Figure 3, the results of the density and mechanical strength analysis are presented. Before the heat treatment, the specimen FA3f had a density of 0.60 g/cm³ and a compressive strength of 1.24 MPa. The high temperature behaviour was first followed by dilatometry (Fig. 4), and then the samples were exposed to elevated temperatures. As can be seen from Figure 4, the sample first gradually shrank from room temperature to 200 °C; after that, it expanded until 600 °C, and subsequently shrank, sharply and significantly. From nearly 700 °C, it started to expand up to 1000 °C. The test has not been conducted up to higher temperatures, but from Figure 6 it can be seen that vitrification takes place between 1000 °C and 1200 °C.
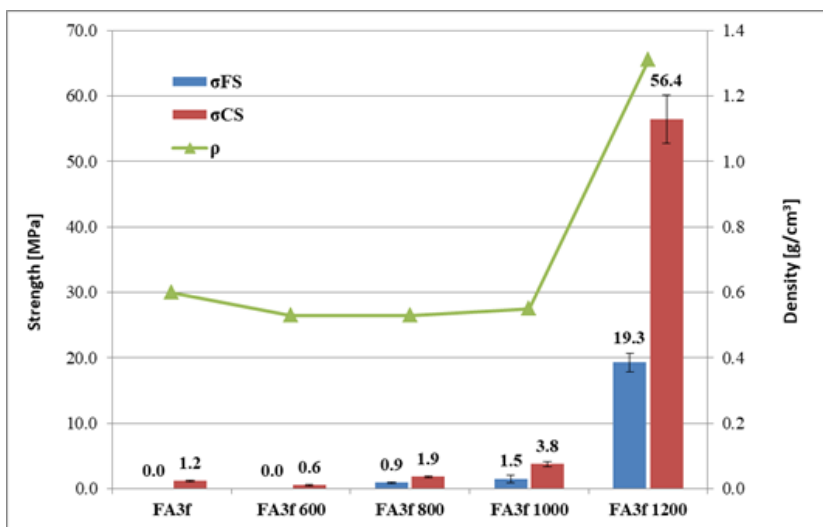

Figure 3: Flexural (σFS) and compressive (σCS) strength and density of the AAF specimens.

After temperature exposure at 600 °C, the density and compressive strength decreased (0.53 g/cm³ and 0.57 MPa, respectively). With increasing temperatures (800 °C and 1000 °C), the density remained almost the same, but the compressive strength began to increase (1.88 MPa and 3.82 MPa, respectively), on account of sintering. The highest shrinkage increment and thus density gain (1.31 g/cm³) appeared at 1200 °C. The sintering leads to Na being directly embodied in glass, implying a loss of efflorescence (Hlavacek *et al.*, 2015). The change in crystalline phases was also detected with XRD (Fig. 5), where there was a decrease in quartz intensity, on the one hand, and on the other, the occurrence of new phases (augite, nepheline, anorthite) was observed. Samples fired at 600, 800 and 1000 °C have practically the same density, but compressive strength increases from 0.6 MPa for the sample fired at 600 °C, to 3.8 MPa for the sample fired at 1000 °C, which could be the result of emerging crystalline phases. After firing at 1200 °C, where densification and vitrification occurs, a significant increase was noticed in flexural and compressive strength (19.29 MPa and 56.42 MPa, respectively). The change in volume and colour of FA3f after temperature exposure is shown in Figure 6 and is in compliance with the measurements discussed above.
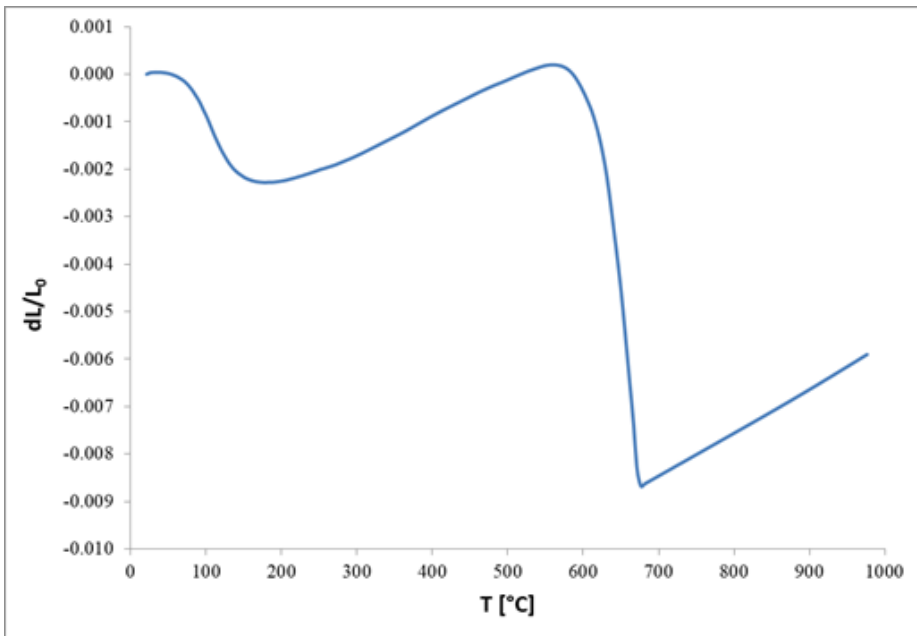

Figure 4: The dL/L₀ as a function of temperature followed by dilatometry.

K. Traven, M. Češnovar, S. Škapin & V. Ducman:
Foundry Wastes as a Potential Precursor in Alkali Activation Technology
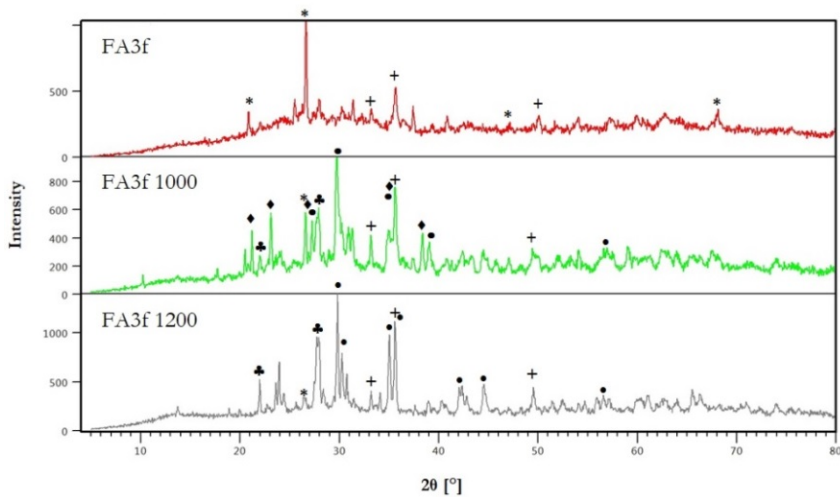
31

Figure 5: X-ray diffractogram of specimens FA3f, FA3f 1000 and FA3f 1200 with the main phases determined and designated as quartz (*), hematite (+), augite (●), nepheline (♦) and anorthite (♣).

Figure 6: AAF specimens before (FA3f) and after (FA3f 600, FA3f 800, FA3f 1000, FA3f 1200) heat treatment.

AAF samples were also investigated by means of SEM. A comparison of images for samples exposed to different temperatures reveals that heat treatment from 600 °C to 1000 °C (Figs. 7 a–d) does not significantly affect the pores, since they are present in all samples, with a diameter ranging from approximately 100 to 450 μm. In

addition, it can be seen that the pores are spherical and uniformly distributed. Also, the effect of pore percolation is observed in all 4 samples. In the case of the FA3f 1200 specimen (Fig. 7e), the average pore diameter decreased to approximately 60 μm, again because of sintering.
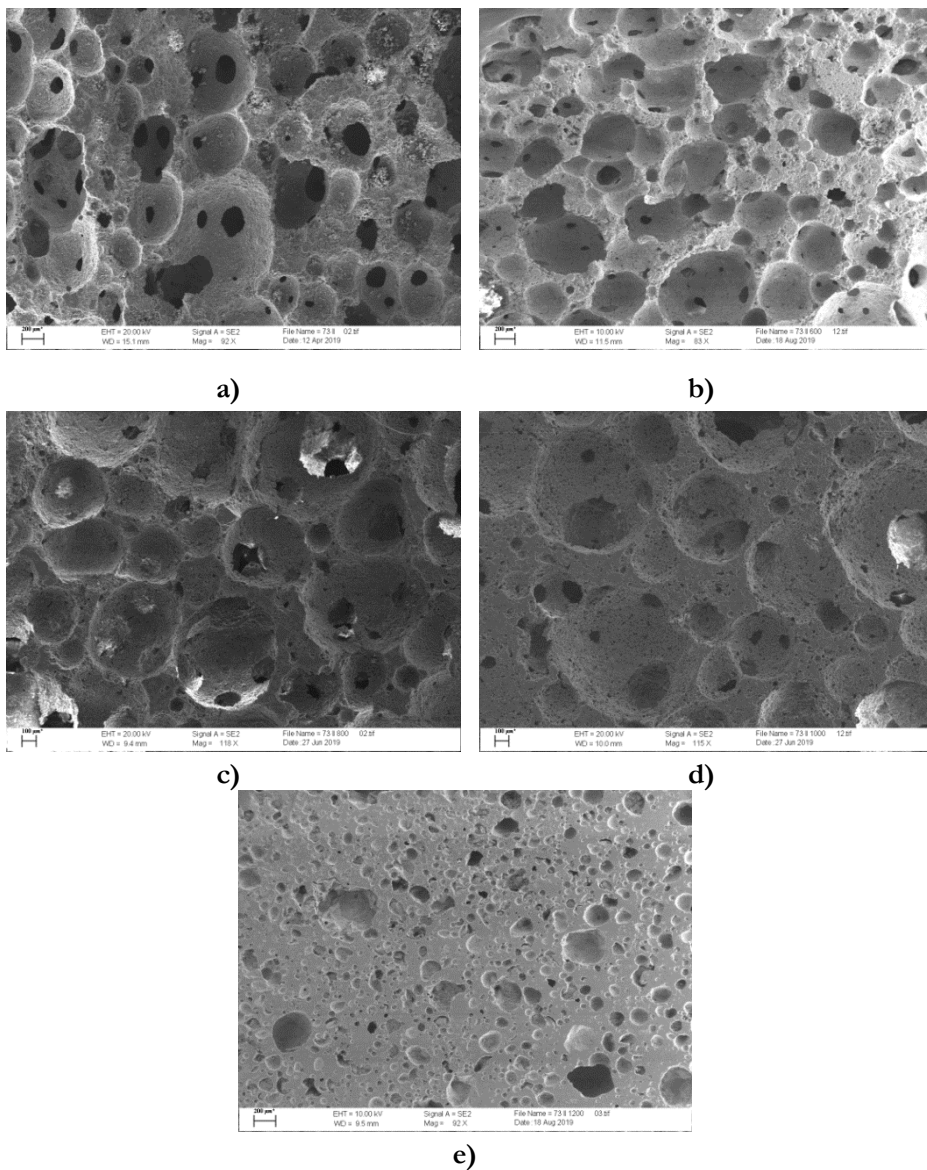
a)

b)

c)

d)

e)

Figure 7: SEM analysis of a) FA3f b) FA3f 600 c) FA3f 800, d) FA3f 1000 and e) FA3f 1200.

K. Traven, M. Češnovar, S. Škapin & V. Ducman:
Foundry Wastes as a Potential Precursor in Alkali Activation Technology

33

4   Conclusions

This study investigated the sustainability of fly ash from a Slovenian power plant as a precursor in an alkali-activation process. The optimal AAM mixture was further used for lightweight AAF development, which resulted in foam with a density of 0.60 g/cm³ and a compressive strength of 1.24 MPa. These specimen samples were later exposed to elevated temperatures (600, 800, 1000 and 1200 °C) to study their dimensional stability, thermal resistance properties and mechanical/microstructural properties after treatment. The following conclusions were made:

–   After exposure to elevated temperatures (600–1000 °C), the density first slightly decreased (0.53 g/cm³) and then significantly increased (1.31 g/cm³) at 1200 °C, because of the sintering process.

–   The mechanical properties are reduced when the sample is exposed to 600 °C. Conversely, the mechanical properties increase after exposure in the range of 800–1200 °C, with the maximum compressive strength reached for the FA3f 1200 specimen at 56.4 MPa.

–   SEM analysis reveals that the pore structures are not affected when heating the specimens to the temperature of 1000 °C; at 1200 °C the pore diameter is significantly reduced.

–   High fire resistance up to 1000 °C enables the use of such AAF in the field of refractory materials.

References

Aiken, T. A., Sha, W., Kwasny, J., Soutsos, M. N. (2017), Resistance of geopolymer and Portland cement based systems to silage effluent attack. *Cement and Concrete Research, 92*, 56-65. doi: https://doi.org/10.1016/j.cemconres.2016.11.015

Bai, C. Y., Colombo, P. (2018). Processing, properties and applications of highly porous geopolymers: A review. *Ceramics International, 44*, 16103-16118. doi: 10.1016/j.ceramint.2018.05.219

Chen, T.-A., Chen, J.-H., Huang, J.-S. (2017). Effects of activator and aging process on the compressive strengths of alkali-activated glass inorganic binders. *Cement and Concrete Composites, 76*, 1-12. doi: 10.1016/j.cemconcomp.2016.11.011

Češnovar, M., Traven, K., Horvat, B., and Ducman, V. (2019). The Potential of Ladle Slag and Electric Arc Furnace Slag use in Synthesizing Alkali Activated Materials; the Influence of Curing on Mechanical Properties. *Materials,* 12, 1-18. doi: https://doi.org/10.3390/ma12071173

Duxson, P., Provis, J. L., Lukey, G. C., Mallicoat, S. W., Kriven, W. M., van Deventer, J. S. J. (2005). Understanding the relationship between geopolymer composition, microstructure and mechanical properties. *Colloid Surface A,* 269, 47-58. doi: 10.1016/j.colsurfa.2005.06.060

Hlavacek, P., Smilauer, V., Skvara, F., Kopecky, L., Sulc, R. (2015). Inorganic foams made from alkali-activated fly ash: Mechanical, chemical and physical properties. *Journal of the European Ceramic Society,* 35, 703-709. doi: 10.1016/j.jeurceramsoc.2014.08.024

Khale, D., Chaudhary, R. (2007). Mechanism of geopolymerization and factors influencing its development: a review. *Journal of Materials Science,* 42, 729-746. doi: 10.1007/s10853-006-0401-4

Korat, L., Ducman, V. (2017). The influence of the stabilizing agent SDS on porosity development in alkali-activated fly-ash based foams. *Cement and Concrete Composites*, 80, 168-174. doi: http://dx.doi.org/10.1016/j.cemconcomp.2017.03.010

Provis, J. L., van Deventer, J. S. J. eds. (2013). *Alkali activated materials: State-of-the-art Report, RILEM TC 224-AAM.* Berlin: Springer/RILEM.

Traven, K., Češnovar, M., Ducman, V. (2019). Particle size manipulation as an influential parameter in the development of mechanical properties in electric arc furnace slag-based AAM. *Ceramics International,* 45, 22632-22641. doi: https://doi.org/10.1016/j.ceramint.2019.07.296

van Deventer, J. S. J., Provis, J. L., Duxson, P. (2012). Technical and commercial progress in the adoption of geopolymer cement. *Minerals Engineering,* 29, 89-104. doi: 10.1016/j.mineng.2011.09.009

Zhang, Z. H., Provis, J. L., Reid, A., Wang, H. (2014). Geopolymer foam concrete: An emerging material for sustainable construction. *Construction and Building Materials,* 56, 113-127. doi: 10.1016/j.conbuildmat.2014.01.081